Highly Conductive Modulation-Doped Graded p-AlGaN/(AlN)/GaN Multi-Heterostructures

Joachim Hertkorn and Zhihao Wu[†]

In this study we present theoretical and experimental results regarding modulation doped p-AlGaN/(AlN)/GaN multi-heterostructures. As the heterostructures should yield both, higher lateral and better vertical conductivity than p-doped GaN, band structure simulations have been performed prior to growth experiments. Based on the simulation results several samples were grown by metalorganic vapor phase epitaxy (MOVPE). High resolution X-ray diffraction was used to determine the effective Al-concentration as well as the period length of the multi-heterostructures. The electrical properties of the samples were investigated by measuring the lateral (σ_L) and vertical (σ_V) conductivity. Moreover electron holography measurements were performed to determine the profile of the valence band. The free hole concentration of a sample optimized in terms of lateral conductivity was measured to be $5.5\times 10^{18}\,cm^{-3}$ (295 K) with a mobility of $12\,cm^2/Vs$, yielding a σ_L of $10\,(\Omega cm)^{-1}$. Low temperature Hall measurements (77 K) proved the existence of a 2DHG at the AlN/GaN interface, as the lateral conductivity could be increased to $25\,(\Omega cm)^{-1}$. By substituting the p-GaN layer in a light emitting diode (LED) with an AlGaN/GaN multi-heterostructure optimized in terms of vertical conductivity, the overall voltage drop could be reduced by more than 100 mV ($j = 65\,A/cm^2$), clearly demonstrating that p-type heterostructures are a candidate to increase the efficiency of high brightness LEDs.

1. Introduction

The research on the III-nitride based technology has developed tremendously during the last few years, yielding a commercialization of many AlGaInN-based devices in several areas. Although the performance of many of those devices is already very impressive, one limiting factor remains the low conductivity of p-type GaN. Due to the relatively high ionization energy of Mg in GaN (170 meV), one has to incorporate very high densities of Mg ($10^{19}\,cm^{-3}$) to achieve reasonable hole concentrations of $\geq 10^{17}\,cm^{-3}$ (295 K). This low hole concentration leads to poor Ohmic contact resistances and a high series resistance of GaN based laser diodes and light-emitting diodes. The high resistivity increases the operating voltage and prevents high driving currents finally limiting the efficacy of the brightest LEDs. At meantime the current spreading in p-GaN layers is limited by the low conductivity also influencing the extraction efficiency of high brightness LEDs. To overcome such problems, the growth of modulation doped p-AlGaN/(AlN)/GaN superlattices

[†]Z. Wu is with the Dept. of Physics, Arizona State University, Tempe, Arizona 85287-1504, USA

is of interest, as high effective hole concentrations of $\geq 10^{18}\,\text{cm}^{-3}$ are achievable in such heterostructures [1–4]. Hereby the strong polarization along the c axis of the GaN crystal and its alloys yields the formation of two-dimensional hole gases at the AlGaN/GaN interface. As the discontinuities of the valence band play an important role regarding this mechanism, the ionization of the Mg atoms is expected to be pushed further by implementing a thin AlN (E_g=6.1 eV) layer at the AlGaN/GaN interface. However the vertical resistivity of such superlattices cannot be neglected, as the use of AlN yields a strong potential barrier for the holes regarding the valence band profile.

2. Band Structure Simulation

To get a better understanding how the AlN might influence the vertical conductivity, we performed band structure calculations by using a classical Schrödinger-Poisson-solver [9] also calculating the local carrier distribution in AlGaN/AlN/GaN heterostructures taking into account the polarization field of the nitride based semiconductors. To keep the influence of the AlGaN on the vertical conductivity as small as possible, we performed simulations with graded Al composition in the AlGaN layer, as proposed by Heikman and Kauser et al. [10, 11]. For all simulations the AlGaN region was assumed to be Mg doped with an atom concentration of $1 \times 10^{19}\,\text{cm}^{-3}$, whereas a background Mg concentration of $5 \times 10^{18}\,\text{cm}^{-3}$ was applied for the nominally undoped GaN.

Based on the results obtained for n-type heterostructures [12] we first carried out simulations without an AlN interlayer at the AlGaN/GaN interface (Fig. 1, left). In such simulations the AlGaN layer was separated into one part with constant Al concentration (AlGaN-barrier) and a second part (20 nm) with a varying Al composition from 0 % near the GaN to 20 % near the AlGaN-barrier. Keeping the period length stable, the GaN and AlGaN-barrier dimensions were varied from 5 nm to 10 nm and 5 nm to 0 nm, respectively.

As the polarization charges are distributed homogeneously over the composition graded region the smooth valence band profile was found to be independent of the AlGaN-barrier thickness (Fig. 1, left). Neglecting this layer it was possible to reduce the period length and the effective Al concentration of the multi-heterostructure, yielding a higher specific

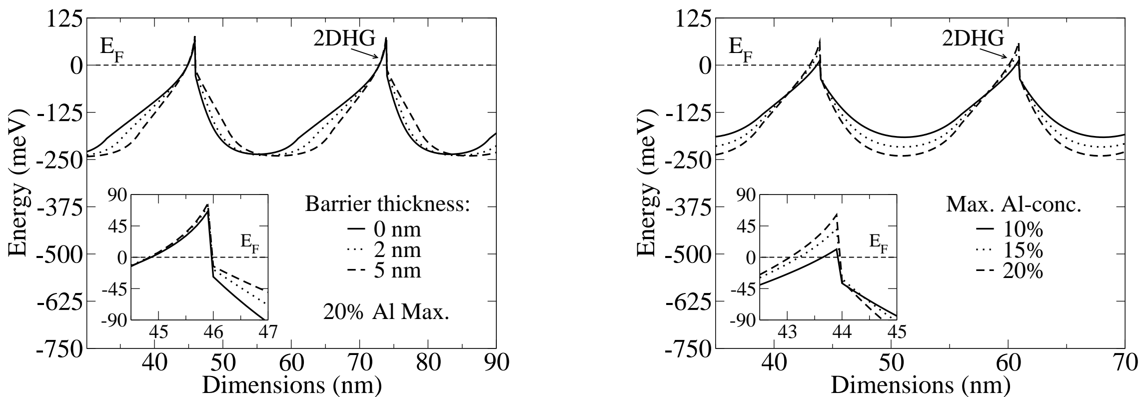

Fig. 1: Influence of the AlGaN-barrier width (left) and the overall Al concentration (right) on the potential profile of the valence band.

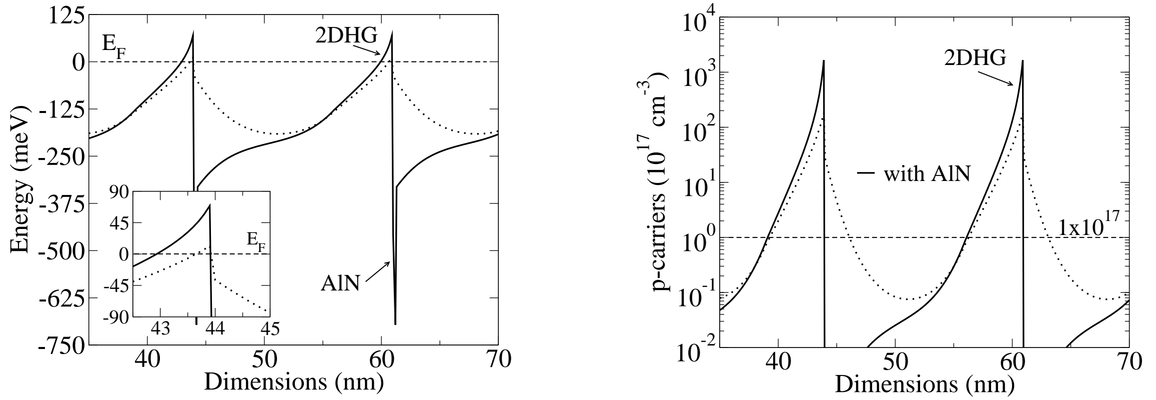

Fig. 2: Band diagram of a structure optimized in terms of lateral conductivity (solid line) and vertical conductivity, respectively.

lateral conductivity and improved strain situation, respectively. The potential barrier of $\approx$ 250 meV in such structures with 20 % Al is expected to have only suboptimal properties in terms of vertical conductivity [10–12]. Therefore simulations were carried out with a reduced Al concentration in the composition graded AlGaN (Fig. 1, right). If the maximum aluminum concentration at the AlGAN/GaN interface was set to 10 % the barrier height was reduced to values of $\approx$ 175 meV (Fig. 1, right, solid line) what should influence the vertical conductivity positively. For the later on performed growth experiments we finally defined such a structure of 12 nm composition graded AlGaN (0 % to 10 %) and 5 nm nominally undoped GaN as the so called "best-vertical" multi-heterostructure.

As the 2DHG carrier concentration is supposed to be negatively influenced by the reduced Al concentration (Fig. 1, right, magnified part) we continued the band structure simulations on "best-vertical" structures including an AlN interlayer ($\approx$ 3 Å) at the AlGaN/GaN interface (Fig. 2, left) finally yielding the so called "best-lateral" structure. The thin interlayer is compensating the disadvantages of the "best-vertical" sample in terms of lateral conductivity, as it can be easily seen in the magnified part in Fig. 2 (left). Using AlN as interlayer, the band discontinuities in the 2DHG region are much stronger (solid line), yielding a higher ionization of acceptors. Thus the carrier concentrations in structures with AlN can be calculated (Fig. 2, right) as high as $5 \times 10^{18}\,\mathrm{cm}^{-3}$ (295 K) whereas the "best-vertical" structure only yields values of $1 \times 10^{18}\,\mathrm{cm}^{-3}$ (295 K). Unfortunately the AlN is expected to be strongly negative for the vertical current flow, as the maximum barrier height is reaching values of about 700 meV.

3. Experimental

Based on the simulation results we worked on optimizing the growth of such low Al containing ($x_{Al} \approx 10\,\%$) and Al graded modulation doped heterostructures with periods of 17 nm by MOVPE. The growth experiments were performed in an AIXTRON 200/RF-S horizontal flow system. The layers were grown on 2" c-plane (0001) epi-ready sapphire wafers slightly miscut by about 0.3° towards the a-plane using an oxygen doped AlN nucleation layer (NL) [5,6]. The process temperature was controlled with a fiber coupled

pyrometer faced to the backside of our rotation tray. All growth temperatures mentioned below are not the real substrate temperatures but the read-out of this pyrometer. Before deposition, the substrates went through in-situ annealing [7] at 1150 °C for 10 min in a hydrogen atmosphere. After the deposition of the NL (≈ 20 nm) and a buffer of around 750 nm undoped GaN, the p-type multi-heterostructures have been grown at a temperature of 1045 °C and a total thickness of around 200 nm. The growth of all layers was performed at a reduced reactor pressure of 100 mbar with the standard precursors trimethyl-aluminum (TMAl), trimethyl-gallium (TMGa), and high purity ammonia (NH_3). As p-type dopant source biscyclopentadienylmagnesium (Cp_2Mg) was applied. The carrier gas was Pd-diffused hydrogen.

The lateral conductivity of the samples was investigated using temperature dependent Van-der-Pauw Hall measurements. To get informations about the implemented amount of Mg atoms, secondary ion mass spectroscopy (SIMS) measurements have been performed. Hence a clear answer could be given how efficient the acceptor ionization in different structures was. To get a feeling for the vertical conductivity of the multi-heterostructures, we grew LEDs with p-type heterostructures in stead of conventional p-GaN and investigated the voltage drop at certain current densities.

The crystallographic properties of the layers were investigated using high resolution X-ray diffraction (HRXRD) and transmission electron microscopy (TEM). To get further informations about the resulting electrostatic potential energy profile of our grown heterostructures we also performed electron holography studies similarly as on our n-type heterostructures [8].

4. Electron Holography

Electron holography is a powerful technique based on TEM to determine the spatial distribution of electrostatic potential with sub-nanometer resolution. For the investigation, performed at the Arizona State University (USA), cross-sectional samples were prepared for electron microscopy using standard mechanical polishing and argon-ion milling techniques. We used a field-effect transmission electron microscope equipped with an electrostatic biprism and operated with incident electron beam energy of 200 keV. Figure 3 (left) shows the phase and amplitude images extracted from a high resolution electron hologram. Due to the limitations in the experimental setup, only the top three periods adjacent to the surface of the heterostructure could be sampled. The electrostatic potential energy profile derived from the phase image is shown on the right hand side of Fig. 3 assuming an electron free mean path of 61 nm for GaN. The boundaries of different regions are carefully determined by a close match with the contrast in the phase image. The 2DHG region occurs at the immediate right of the AlN layer, with a positive curvature and energy rise of ≈ 0.3 eV. In the graded AlGaN layer, the potential energy has an overall negative curvature that may be due to the nonlinear grading of the Al composition in the AlGaN layer and/or to a net negative charge density. The charge density in the AlGaN is a sum of two components: the negative (ionized) acceptor density N_A^- in the AlGaN and the polarization charge density, due to the gradient in polarization associated with the Al compositional grading. In addition, many tiny bumps with negative

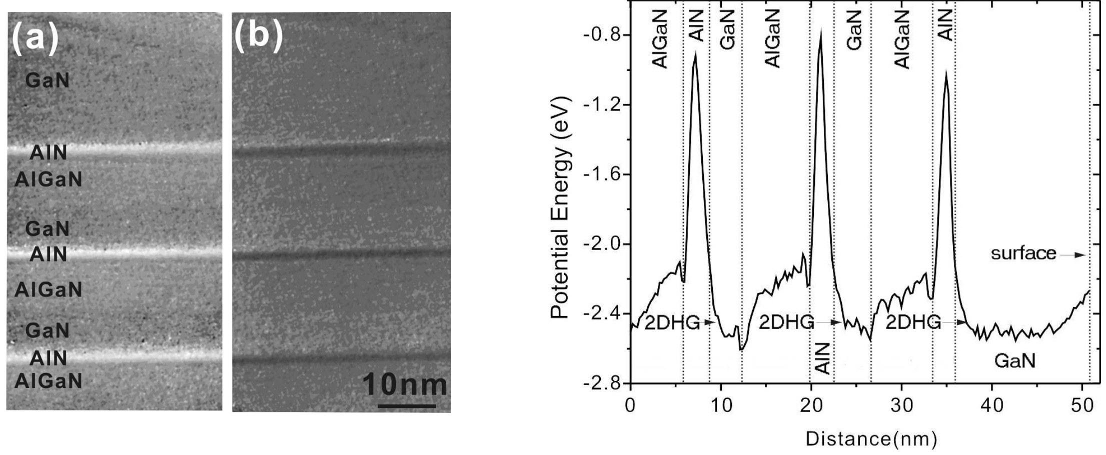

Fig. 3: Phase (a) and amplitude image (b) of a "best-lateral" heterostructure extracted from an electron hologram (left). Potential energy profile across the multi-heterostructure (right), derived from (a) and (b), assuming an inelastic mean-free path of 61 nm for GaN.

curvature have been observed in AlGaN, which could be due to the uneven doping of Mg, assuming the Al composition is smoothly varied. In order to compare the obtained potential energy profile with the valence band diagram, it is necessary to clarify the difference and relationship between these two profiles. For a material with constant composition like GaN, the electrostatic potential variation is identical to the energy band variation; but for a compositionally graded material like $Al_xGa_{1-x}N$, the measured mean inner potential (MIP) difference with reference to GaN varies as $\Delta MIP(x) = 2.59\,x$, while the conduction band offset varies as $\Delta E_c(x) = 1.78\,x$ and the valence band profile varies as $\Delta E_v(x) = -0.89\,x$. Therefore, in the electrostatic potential energy the AlN layer is visible as a spike with abrupt energy steps at the interfaces. Regions with higher Al composition in the graded AlGaN exhibit higher potential energy value. From Fig. 3 (right) the MIP difference between GaN and the highest Al composition AlGaN in graded AlGaN is about 0.4 eV, indicating the highest Al composition is about 15 %, which will lead to a valence band offset of -0.135 eV. Thus, the energy barrier in the graded AlGaN sensed by the holes will be around 0.135 eV, a value matching the simulation (175 meV) quite well. To get an answer if the free carrier concentration is as well in agreement with the simulation, we investigated the electrical properties of the samples.

5. Electrical Properties

Based on the band structure simulations we have defined two kinds of samples optimized in terms of either good vertical ("best-vertical") or high lateral ("best-lateral") conductivity (see section 2). Although the simulation gave us a clear theoretical indication about the structural design parameters, the Mg memory effect in MOVPE systems is limiting the abruptness of modulation doping, and thus the performance of p-type heterostructures [13]. By an optimization of the growth conditions, we could partly overcome such problems as investigated by SIMS. A homogeneous Mg profile from the first to the last period of the superlattice could be achieved, what is important for a clear interpretation

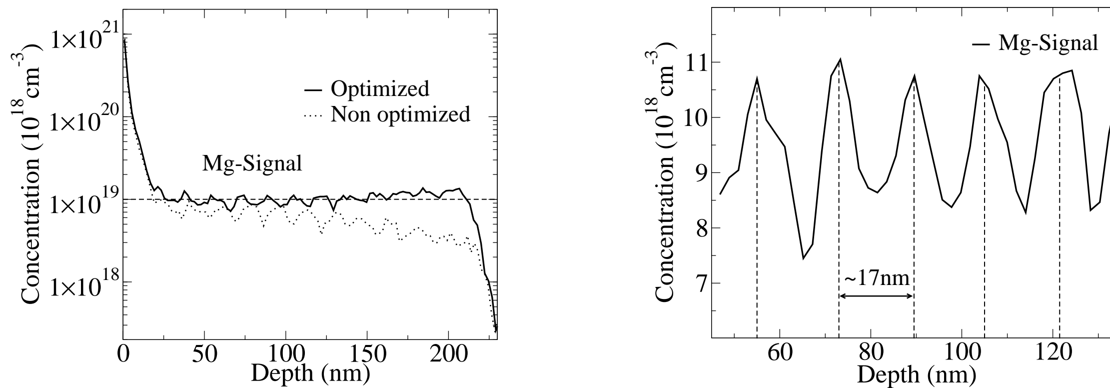

Fig. 4: On the left hand side two SIMS spectra of multi-heterostructures designed for high lateral conductivity ("best-lateral") are shown. On the right hand side it is indicated on a linear scale that the modulation doping in the multi-heterostructures is limited by the Mg memory effect.

of the later on performed Hall measurements. On the left hand side of Fig. 4 it is clearly visible, that the averaged Mg concentration is stable at a value of about $1 \times 10^{19}\,\mathrm{cm}^{-3}$ over the whole layer of heterostructures whereas the modulation doping is limited by the Mg memory effect (Fig. 4, right). Prior to the Hall measurements the p-carriers were activated for 60 sec by an annealing step reaching a maximum temperature of about 750 °C. As contacts we used In bumps annealed at around 500 °C for 20 sec yielding ohmic behavior. The activation as well as the contact annealing were performed in air. The free hole concentrations of a "best-lateral" structure was measured to be $5.5 \times 10^{18}\,\mathrm{cm}^{-3}$ (295 K) with a mobility of $12\,\mathrm{cm}^2/\mathrm{Vs}$, yielding a lateral conductivity of $10\,(\Omega\mathrm{cm})^{-1}$. Thus the experimentally determined values fitted quite well to the simulation results. Low temperature Hall measurements (77 K) proved the existence of a 2DHG at the AlN/GaN interface, as the conductivity could be increased to $25\,(\Omega\mathrm{cm})^{-1}$. Here the carrier concentration remained almost constant ($4.8 \times 10^{18}\,\mathrm{cm}^{-3}$) and the mobility increased to values of about $30\,\mathrm{cm}^2/\mathrm{Vs}$. The result of a temperature dependent Hall-measurement of the "best-lateral" sample can be seen in Fig. 5. With higher temperatures the ionization of all acceptor occurs and the free hole concentration is reaching values of $1 \times 10^{19}\,\mathrm{cm}^{-3}$ as expected from SIMS measurement.

In "best-vertical" samples we could only achieve lateral conductivities of $2.5\,(\Omega\mathrm{cm})^{-1}$ (295 K), as the ionization was remarkably lower due to the missing AlN interlayer. The carrier concentration dropped dramatically to values of about $2.4 \times 10^{18}\,\mathrm{cm}^{-3}$. Moreover the alloy disorder scattering of the holes reduced the mobility to values of about $6\,\mathrm{cm}^2/\mathrm{Vs}$.

Another proof of the perfect abruptness of the AlN/GaN-interface is given by HRXRD. The omega-2-theta scan (Fig. 6) clearly resolves the 10 fringes of the multi-heterostructure (12 periods, "best-lateral") at the low and high-angle side of the main GaN peak. Assuming completely strained growth the effective Al concentration was evaluated to be in the range of 7 %. As the theoretically calculated value is 5.5 % we can conclude, that the Al concentration is somewhat higher than expected and/or the linear grading of the Al flow during epitaxial growth yields a parabolic composition grading, as already observed in our n-type heterostructures [8] and indications from TEM holography (sec. 4).

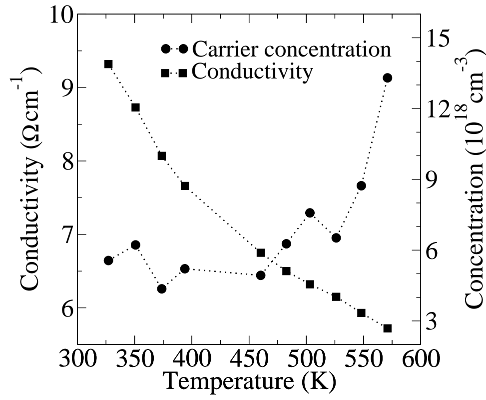

Fig. 5: Temperature dependent Hall measurement of the "best-lateral" sample.

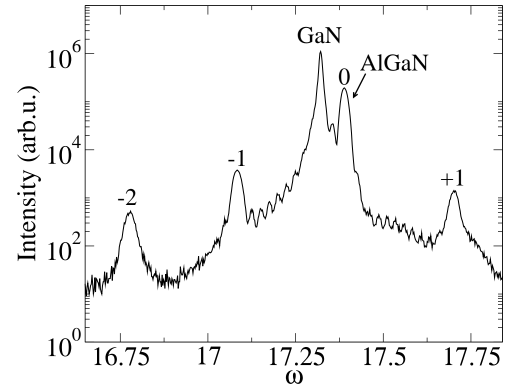

Fig. 6: X-ray diffraction (ω-2Θ) profile of an AlGaN/AlN/GaN multi-heterostructure.

In order to investigate the performance in terms of vertical conductivity, we grew three types of LEDs, one with a conventional p-GaN layer and two where the p-GaN layer was substituted by a "best-lateral" or a "best-vertical" structure, respectively. Regarding σ_V we just concentrated on the absolute voltage drop at current densities of 65 A/cm^2. The layer thickness of the p-side was either 170 nm for the LEDs with multi-heterostructures or 110nm for normal p-GaN. The lowest voltage drop was observed in the LED with "best-vertical" structure, whereas the LED with p-GaN and "best-lateral" structure showed a 4.5 % or 6 % higher power dissipation, respectively. Thus p-type AlGaN/(AlN)/GaN superlattices seem to be a candidate to increase the efficiency of high brightness LEDs.

6. Conclusion

In this study we demonstrated the experimental realization of p-type AlGaN/GaN heterostructures yielding improved vertical and lateral conductivities compared to conventional p-GaN. Such heterostructures seem to be an ideal candidate to increase the efficiency of high brightness LEDs. Prior to growth experiments band structure simulations have been performed yielding the layer profile of the heterostructure. Electron holography measurements yielded results in good agreement to the simulations.

7. Acknowledgment

This research was financially supported by Osram Opto Semiconductors and the Bundesministerium für Bildung und Forschung (BMBF). The sample characterization by K. Forghani, A. Grob, H. Kaim and S. Galichin, MicroGaN GmbH (Hall-Data) and IAF-Freiburg (SIMS) is gratefully acknowledged.

References

[1] E. F. Schubert, W. Grieshaber and I. D. Goepfert, *Appl. Phys. Lett.*, vol. 69, no. 24, pp. 3737-3739, 1996.

[2] L. Hsu and W. Walukiewicz, *Appl. Phys. Lett.*, vol. 74, no. 17, pp. 2405-2407, 1999.

[3] P. Kozodoy, Y. P. Smorchkova, M. Hansen, H. Xing, S. P. DenBaars, U. K. Mishra, A. W. Saxler, R. Perrin and W. C. Mitchel, *Appl. Phys. Lett.*, vol. 75, no. 16, pp. 2444-2446, 1999.

[4] A. Y. Polyakov, N. B. Smirnov, A. V. Govorkov, A. V. Osinsky, P. E. Norris, S. J. Pearton, J. Van Hove, A. M. Wowchack and P. P. Chow , *J. Appl. Phys.*, vol. 90, no. 8, pp. 4032-4038, 2001.

[5] B. Kuhn, F. Scholz, *phys. stat. sol. (a)*, vol. 188, no. 2, pp. 629-633, 2001.

[6] J. Hertkorn, P. Brückner, S.B. Thapa, T. Wunderer, F. Scholz, M. Feneberg, K. Thonke, R. Sauer, M. Beer, J. Zweck, *J. Crystal Growth*, vol. 308, pp. 30-36, 2007.

[7] J.-H. Kim, S.C. Choi, K.S. Kim, G.M. Yang, C.-H. Hong, K.Y. Lim, H.J. Lee, *Jpn. J. Appl. Phys.*, vol. 38, no. 5A, pp. 2721-2724, 1999.

[8] Z. H. Wu, F. A. Ponce, J. Hertkorn, F. Scholz, *Appl. Phys. Lett.*, vol. 91, no. 14, pp. 142121-1 - 142121-3, 2007.

[9] M. Grundmann, University of California, Santa Barbara, (http://my.ece.ucsb.edu/mgrundmann/bandeng.htm).

[10] S. Heikman, S. Keller, D. S. Green, S. P. DenBaars and U. K. Mishra, *J. Appl. Phys.*, vol. 94, no. 8, pp. 5321-5325, 2003.

[11] M. Z. Kauser, A. Osinsky, A. M. Dabiran, P. P. Chow, *Appl. Phys. Lett.*, vol. 85, no. 22, pp. 5275-5277, 2004.

[12] J. Hertkorn, P. Brückner, C. Gao, F. Scholz, A. Chuvilin, U. Kaiser, U. Wurstbauer, W. Wegscheider, *phys. stat. sol. (c)*, vol. 5, no. 6, pp. 1950-1952, 2008.

[13] E. L. Waldron, J. W. Graff, E. F. Schubert, *Appl. Phys. Lett.*, vol. 79, no. 17, pp. 2737-2739, 2001.